OPEN ACCESS

University of BRISTOL

Pickering, R., Cassarino, L. A., Hendry, K., Wang, X., Maiti, K., & Krause, J. (2020). Using Stable Isotopes to Disentangle Marine Sedimentary Signals in Reactive Silicon Pools. *Geophysical Research Letters*, *47*(15), [e2020GL087877]. https://doi.org/10.1029/2020GL087877

Publisher's PDF, also known as Version of record

Link to published version (if available):
10.1029/2020GL087877

Link to publication record in Explore Bristol Research
PDF-document

University of Bristol - Explore Bristol Research
General rights

Geophysical Research Letters

Key Points:
- We quantified δ^{30}Si values for operationally defined reactive Si pools in coastal sediments, describing previously hidden δ^{30}Si values for the first time
- The isotopic shift is drastic, as the δ^{30}Si of Si liberated in the acid preleach is 4.5–5‰ lower than that of traditional and sequential sodium carbonate digestions
- A likely pathway of formation for the isotopically light material found in the acid preleach is a single-step fractionation of an already light isotopic source

Author Contributions:
Conceptualization: Rebecca A. Pickering, Jeffrey W. Krause
Formal analysis: Rebecca A. Pickering, Lucie Cassarino, Katharine R. Hendry, Xiangli L. Wang, Kanchan Maiti, Jeffrey W. Krause
Investigation: Rebecca A. Pickering, Kanchan Maiti, Jeffrey W. Krause
Supervision: Rebecca A. Pickering, Jeffrey W. Krause
Writing - original draft: Rebecca A. Pickering, Lucie Cassarino, Katharine R. Hendry, Xiangli L. Wang, Kanchan Maiti, Jeffrey W. Krause
Writing – review & editing: Rebecca A. Pickering, Lucie Cassarino, Katharine R. Hendry, Xiangli L. Wang, Kanchan Maiti, Jeffrey W. Krause

Using Stable Isotopes to Disentangle Marine Sedimentary Signals in Reactive Silicon Pools

Rebecca A. Pickering[1,2] 🆔, Lucie Cassarino[3] 🆔, Katharine R. Hendry[3] 🆔, Xiangli L. Wang[2,1], Kanchan Maiti[4], and Jeffrey W. Krause[1,2] 🆔

[1]Dauphin Island Sea Laboratory, Dauphin Island, AL, USA, [2]Department of Marine Sciences, University of South Alabama, Mobile, AL, USA, [3]School of Earth Sciences, University of Bristol, Bristol, UK, [4]Department of Oceanography and Coastal Studies, Louisiana State University, Baton Rouge, LA, USA

Abstract Many studies use sedimentary biogenic silica ($bSiO_2$) stable isotopes (e.g., δ^{30}Si) as paleoproxies but neglect signals from other sedimentary reactive SiO_2 phases. We quantified δ^{30}Si for multiple reactive Si pools in coastal river-plume sediments, revealing up to −5‰ difference between acid-leachable and alkaline-digestible amorphous SiO_2. Thus, previous studies have missed valuable information on early diagenetic products and, in cases where sediments were not cleaned, potentially biased $bSiO_2$ δ^{30}Si values. Acid-leachable δ^{30}Si, that is, from authigenic products, are the result of either multistep fractionation from a $bSiO_2$ source or an ~2‰ fractionation (consistent with metal hydroxide formation) from slowly dissolving lithogenic SiO_2. This analysis also suggests that sedimentary diatom $bSiO_2$, which has increased regionally in the last half-century, is the critical substrate of early authigenic Si precipitates. Regional eutrophication, which has stimulated sedimentary $bSiO_2$ accumulation, may have facilitated additional sequestration of both sedimentary Si and cations from early diagenetic products.

Plain Language Summary A growing body of scientists use the isotopic signatures in silica like chemical fingerprints to understand how biologic organisms functioned during the past; however, these methods typically neglect potentially useful information from nonbiological silica phases. We measured silica signals for multiple phases in coastal sediments, discovering a large isotopic differences between phases formed abiotically in sediments and biologic silica deposited from the overlying waters. These newly formed silica phases are the result of either a large isotopic shift from biological sources or a smaller shift from slowly dissolving mineral silica. Additionally, these data reveal that biological silica is an important surface for the newly produced silica phases to form. The increased regional biogenic silica burial, coincident with eutrophication since the mid-20th century, may have had an additive effect on increasing the sequestration of silica and other bioreactive elements in these sediments.

1. Introduction

The weathering of silicate minerals and secondary formation of authigenic silicate phases both regulate elemental cycling and the Earth's climate (Isson & Planavsky, 2018; Sutton et al., 2018). The relative abundances of silicon (Si) stable isotopes (^{28}Si [92.2%], ^{29}Si [4.7%], and ^{30}Si [3.1%]) have been used to estimate carbon export rates, reconstruct silicate weathering, and determine both global and coastal sources/sinks of sedimentary Si (Frings et al., 2016; Opfergelt & Delmelle, 2012; Trower & Fischer, 2019). Because diatoms account for a significant proportion of marine primary production, stable Si isotope compositions (e.g., δ^{30}Si, defined as ^{30}Si/^{28}Si relative to a standard) in sedimentary biogenic silica ($bSiO_2$) are widely used as a paleoproxy for marine silicic acid usage by pelagic diatoms (Sutton et al., 2018).

Despite the growing body of work that uses sedimentary $bSiO_2$ δ^{30}Si signals to reconstruct the past (Frings et al., 2014, 2016), none of these studies report δ^{30}Si data on other operational Si reactive pools (amorphous silica phases) in sediments. Michalopoulos and Aller (2004) demonstrated that early authigenic products could be estimated by examining multiple amorphous sedimentary Si pools including traditionally measured $bSiO_2$. Operational reactive Si pools previously defined in the literature (DeMaster, 1981; Krause et al., 2017; Michalopoulos & Aller, 2004; Qin et al., 2012; Rahman et al., 2016; Wang et al., 2015) include (1) mild acid-leachable highly reactive silica associated with authigenic products, for example, metal oxide coatings (Si-HCl); (2) mild alkaline-leachable digested silica after acid pretreatment associated with authigenically

altered and unaltered $bSiO_2$ (Si-Alk); (3) NaOH soluble silica following Steps 1 and 2 associated with soluble lithogenic Si (LSi) and remaining refractory $bSiO_2$, for example, sponge spicules and polycystine radiolarians (Si-NaOH); and (4) traditional mild alkaline-leachable sedimentary $bSiO_2$, with no acid pretreatment, which does not account for $bSiO_2$ which has undergone authigenesis (T-$bSiO_2$). As the use of $\delta^{30}Si$ signals to understand early diagenesis grows, it has become evident that we lack understanding about these other reactive Si pools. Previous studies examining $\delta^{30}Si$ in marine sediments have just focused on traditional $bSiO_2$ alkaline-digestions (Ehlert et al., 2016; Frings et al., 2014, 2015, 2016; Ziegler, Chadwick, White, et al., 2005). Though there are a number of studies utilizing the Michalopoulos and Aller (2004) sequential extraction methodology (Krause et al., 2017; Presti & Michalopoulos, 2008; Qin et al., 2012; Wang et al., 2015), these studies lack $\delta^{30}Si$ data.

Isotopic characterization of operationally defined pools could provide a critical constraint on reactive silica budgets. Potentially important diagenetic information is being missed by not quantifying the Si isotopes of early authigenic products (e.g., metal hydroxides). Previously, natural radioactive ^{32}Si was used to examine these operational pools (Rahman et al., 2016, 2017) and led to the first global estimates of marine secondary clay production—estimated to be 4.5–4.9 Tmol Si yr^{-1} (Rahman et al., 2017). This estimate partially closes gaps in the marine Si budget between global Si ocean inputs, but a gap upward of 1.1 Tmols Si yr^{-1} still remains (Frings et al., 2016; Maldonado et al., 2019; Rahman et al., 2019; Tréguer & De La Rocha, 2013). Traditional estimates of $bSiO_2$ reservoirs in marine sediments are based on diatom frustules (Tréguer & De La Rocha, 2013), although more recent studies (Maldonado et al., 2019) suggest that refractory $bSiO_2$ (e.g., sponge spicules), which is conventionally missed by short-duration alkaline digestions, may account for an ~1.7 Tmol Si yr^1 global Si burial sink. Including this "dark $bSiO_2$" brings the global Si ocean budget closer to equilibrium, but not necessarily in balance.

This study lays the groundwork for examining reactive Si pools in coastal sediments and examining their stable Si isotopic composition (instead of ^{32}Si), shedding light on the potential mechanisms behind reactive silica formation. We report $\delta^{30}Si$ of operationally defined reactive Si pools in coastal Mississippi River plume sediments using a sequential alkaline digestion following a mild acid leach. We report an exceptionally isotopically light sedimentary Si pool associated with early diagenetic transformation of Si. The isotopically light Si ($-2.89 \pm 0.45‰$) in these early authigenic products is the result of either exceptional fractionation (up to 5‰) from a $bSiO_2$ source in sediments or a 2‰ fractionation (consistent with metal hydroxide formation) from the slowly dissolving silica pool largely dominated by lithogenic material. Furthermore, diatom frustules (which are isotopically heavy) are inferred to be a critical substrate for the formation of these isotopically light authigenic precipitates. This finding has major implications on Si and cation sequestration in coastal plume sediments globally, especially in light of increased $bSiO_2$ accumulation associated with eutrophication.

2. Materials and Methods

2.1. Study Sites

Short (<0.5 m) sediment cores were collected during spring 2017 at three stations: A7 (28.947°N, −89.750°E), C6 (28.865°N, −90.495°E), and D5 (28.499°N, −90.835°E) (Figure S1 in the supporting information). These sites are on the coastal Louisiana shelf in the northern Gulf of Mexico and are affected by the Mississippi River plume but not west enough to be affected by the Atchafalaya River. Briefly, samples were acquired using an Ocean Instruments MC-900 Multi-corer, which preserves the sediment-water interface during recovery. Overlying bottom water was removed, cores were sectioned into 1-cm slices, homogenized, packed under N_2 gas, and frozen at −20°C for further analysis.

2.2. Reactive Silica Pools

Frozen sediment samples were thawed to room temperature (22°C), and triplicate ~50- to 100-mg subsamples were weighed into 50-ml polyethylene centrifuge tubes. Samples were never dried or ground prior to and during extractions. Procedural blanks were also prepared in triplicate. Additional subsamples were dried at 60°C to determine water content. The sequential extraction methodology separates silica into operationally defined pools based on kinetics, reaction conditions, and reaction sequence (DeMaster, 1981; Michalopoulos & Aller, 2004; Rahman et al., 2016). One-milliliter aliquot of each resulting leach
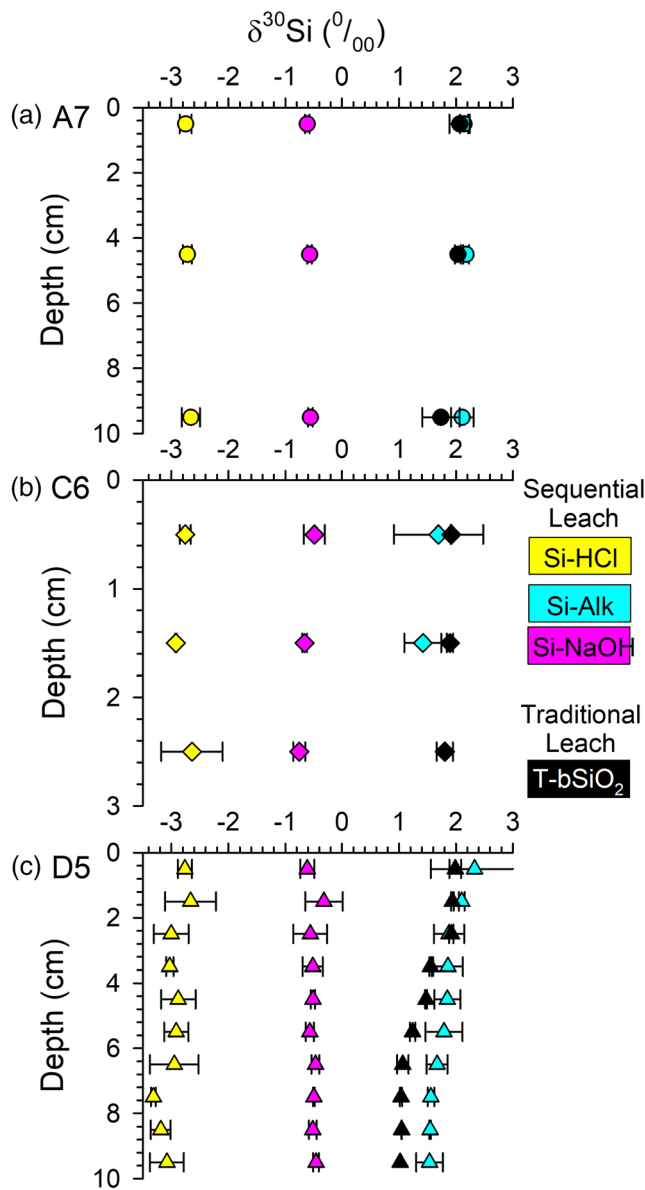
Figure 1. Reactive δ^{30}Si signals. Comparative average ($\pm 2\sigma$) ($n = 3$) δ^{30}Si (‰) signals among reactive Si pools using a sequential multistep (Si-HCl, Si-Alk, and Si-NaOH) digestion and traditional (T-bSiO$_2$) alkaline-only extraction methodologies at varying depths from three short sediment cores (<0.5 m). (a–c) Cores (C6, D5, and A7) were collected within the coastal Louisiana shelf in the northern Gulf of Mexico and contain Mississippi River plume sediments. Error bars are present for each point but may be obscured as error is smaller than symbol size. Note change in depth (cm) scale on *y* axis for each core.

(Si-HCl, Si-Alk, Si-NaOH, and T-bSiO$_2$) was analyzed for dissolved Si (OH)$_4$ concentration using a spectrophotometric molybdate-blue method (Brzezinski & Nelson, 1986). Supernatants for stable isotope analysis were concentrated via evaporation at 100°C and stored until purification and mass spectrometer analysis.

2.2.1. Acid-Leachable Silica (Si-HCl)

Sediment extractions were run at room temperature (22°C) using 36-ml 0.1 N HCl (Honeywell Fluka™ Trace SELECT™) for 18 hr, while keeping particles suspended (shaker table). This resulted in a sediment dry weight solid-to-solution ratio (SSR) of ~0.7–1.4. Following centrifugation, the Si-HCl leachate was removed and neutralized with 4 N NaOH to pH 7. The leachate was analyzed for both silica content and silicon isotopes. Remaining sediment was rinsed in triplicate with Milli-Q (18.2 MΩ * cm) water to remove any residual acid (Michalopoulos & Aller, 2004). Rahman et al. (2016) demonstrated these rinses contained minor amounts of Si, and they were discarded. A weak HCl molarity was purposely chosen to remove metal coatings, authigenic phases, and activate bSiO$_2$ surfaces while not affecting the sequential Si-Alk digestion (Michalopoulos & Aller, 2004).

2.2.2. Mild Alkaline-Leachable Si (Si-Alk) and Traditional bSiO$_2$ Digestion (T-bSiO$_2$)

The remaining sediment from the acid pretreatment was subsequently digested with 25-ml 0.1 M Na$_2$CO$_3$ (Fisher Scientific™ Certified ACS) (dry weight SSR ~ 1–2) in an 85°C water bath; digestions were run up to 5 hr. Following 20 min, subsamples were neutralized with 1 N HCl to stop the digestion (final pH: 7). This timepoint was within error of the traditional intercept from a regression of individual timepoints (Table S1), ensuring the absence of significant lithogenic material (DeMaster, 1981; Michalopoulos & Aller, 2004). Thus, the clear majority of solubilized silica was biogenic, and this timepoint was used for all further analyses and data manipulation. Other time points (through 5 hr) were subsampled according to the standard approach (DeMaster, 1981). After 5 hr, the material was centrifuged and the leachate was removed and discarded. Remaining sediment was rinsed in triplicate with Milli-Q water to remove any residual Na$_2$CO$_3$, and again the rinses were discarded. A second sample subset was analyzed following the traditional sediment bSiO$_2$ method (DeMaster, 1981). The sampling frequency and digestion duration was exactly the same as for Si-Alk but with no acid pretreatment (denoted as T-bSiO$_2$).

2.2.3. Harsh NaOH Digestion (Si-NaOH)

The remaining sediment from the Si-Alk treatment was subsequently digested with 10-ml 4 M NaOH (Honeywell Fluka™) (dry weight SSR ~ 2.5–5) for 2 hr in an 85°C water bath. After 2 hr, samples were neutralized with 10 N HCl to stop the digestion (final pH: 7). Following centrifugation, the Si-NaOH leachate was removed, the remaining sediment was rinsed with Milli-Q water to remove any residual leachate, and this rinse was added to the Si-NaOH leachate and stored for further analysis as done previously (Rahman et al., 2016). This digested material was analyzed for both silica content and silicon isotopes.

2.3. Stable Isotope Analysis

Sample purification and isotope analysis were carried out at the University of Bristol Isotope Group laboratories. Concentrated sample fluids were purified via cation exchange chromatography (Bio-Rad
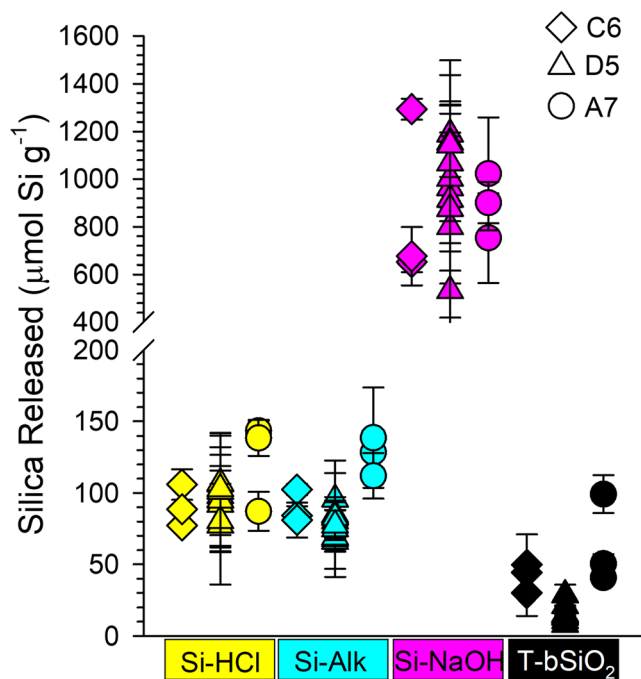
Figure 2. Reactive Si mass differential. Average ($\pm 2\sigma$) ($n = 3$) silica released (μmol Si per g sediment) during reactive Si pool extractions. Core locations denoted by symbol shape.

AG50W-X12, 200-400 mesh cation exchange resin in H$^+$ form) following Georg et al. (2006). A detailed description of purification steps is included in the supporting information (Text S1). Purified solutions (2–3 ppm Si) were analyzed in duplicate for Si isotopes (^{28}Si, ^{29}Si, and ^{30}Si) using a multicollector-inductively coupled plasma-mass spectrometer (MC-ICP-MS, Finnigan Neptune s/n 1002), equipped with CETAC PFA spray chamber and PFA nebulizer (100 μl min^{-1}). A standard-sample-standard bracketing procedure with Mg doping following Cardinal et al. (2003) was used to correct for both instrumental mass bias and potential matrix effects. Additionally, sample and standard solutions were both doped with 0.1 M H$_2$SO$_4$ (ROMIL UpA) and 1 M HCl (in-house distilled) to reduce any potential matrix effects from anion loading and guarantee matrix matching between sample and standard (Hughes et al., 2011). All isotopic composition results are expressed as δ^{30}Si, corresponding to the silicon isotopic abundances in samples relative to the international reference standard NBS-28 (NIST RM8546, purified quartz sand). Reference standards Diatomite (Reynolds et al., 2007) and LMG08 (sponge) (Hendry et al., 2011) were run in tandem with samples to assess long-term reproducibility. Average measured values are reported as $+1.27 \pm 0.09$‰ ($n = 75$) and -3.47 ± 0.16‰ ($n = 27$) ($\pm \sigma$), respectively, which are well within agreement with published values (Hendry et al., 2011; Reynolds et al., 2007). All samples and standards are consistent with the kinetic mass fractionation law (Reynolds et al., 2007) with the δ^{29}Si $= 0.518 \times \delta^{30}$Si. Procedural blanks were lower than the detection limit and thus considered negligible on δ^{30}Si of the samples.

2.4. Lithogenic Corrections

Both Si-Alk and T-bSiO$_2$ δ^{30}Si signals (‰) and mass of Si released (μmol g^{-1}) were adjusted for bias from lithogenic material following Kamatani and Oku (2000) and Ragueneau et al. (2005). Further details included in the supporting information (Text S2). T-bSiO$_2$ corrections were insignificant (0.00 μmol g^{-1}) due to the absence of significant lithogenic material.

3. Results

The δ^{30}Si differences among the operational pools were drastic and revealed some of the most isotopically light Si observed in the ocean (Figure 1). δ^{30}Si$_{HCl}$ signals ranged from -3.34‰ to -2.61‰ with an average of -2.89 ± 0.45‰ ($\pm 2\sigma$) ($n = 48$). These values are similar to groundwater silcretes, with a mean δ^{30}Si of -3.8‰ (Basile-Doelsch, 2006; Basile-Doelsch et al., 2005) and significantly lighter than previous oceanic sedimentary bSiO$_2$ (-1‰ to $+2$‰; Frings et al., 2016; Sutton et al., 2018). The δ^{30}Si composition of this acid-leachable pool is 4.5–5‰ lower than that of the silica associated with biosiliceous organisms like diatoms, rhizaria, and sponges (Si-Alk, includes authigenically altered silica; T-bSiO$_2$, no authigenically altered silica, Figure 1). However, there are also differences between the isotopic composition of the Si-Alk and T-bSiO$_2$ pools (Figure 1). δ^{30}Si$_{T-bSiO2}$ among all cores and depths averaged $+1.63 \pm 0.39$‰ ($\pm 2\sigma$) (range: $+1.00$‰ to $+2.19$‰) ($n = 32$) and δ^{30}Si$_{Alk}$ values averaged $+1.84 \pm 0.59$‰ ($\pm 2\sigma$) (range: $+1.23$‰ to $+2.69$‰) ($n = 48$). Overall, the traditional digestion (T-bSiO$_2$) average was significantly lower than δ^{30}Si$_{Alk}$ by 0.21‰ (ANOVA, $p = 0.007$). This overall difference was not monotonic among cores; two cores (D5 and A7 had ANOVA, p values of <0.001 and 0.029, respectively) showed significant differences, whereas one did not (C6, $p = 0.066$). Additionally, while δ^{30}Si$_{Alk}$ of Core C6 was ($p = 0.066$) different than δ^{30}Si$_{T-bSiO2}$, this difference is in opposition to Cores D5 and A7, with Si-Alk signals 0.23‰ lower than T-bSiO$_2$. Excluding Core C6, the overall differences between Si-Alk and T-bSiO$_2$ remain significant (ANOVA, $p = 0.002$), implying that spatial variation, organic content, and sediment type influence the magnitude of difference between the isotopic composition of these Si pools to some degree. The mass (μmol g^{-1}) of Si released from Si-Alk (includes authigenically altered bSiO$_2$) was between 2 and 9 times larger than that of
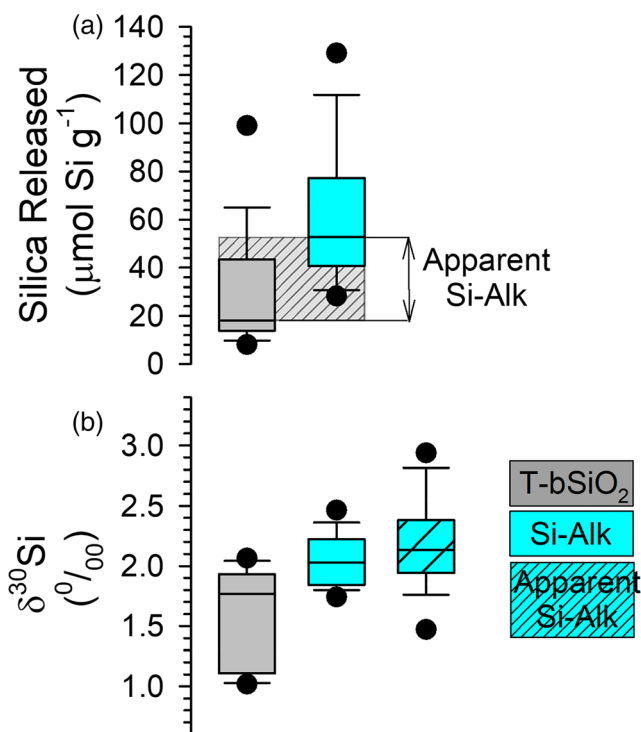
Figure 3. Authigenically altered bSiO$_2$. (a) Apparent Si-Alk (μmol Si per g sediment) mass of Si released and (b) Apparent Si-Alk δ^{30}Si (‰) values comparative to Si-Alk and T-bSiO$_2$ values from biogenic pools. Apparent Si-Alk is the "new" authigenically altered bSiO$_2$ liberated in the Si-Alk digestion, relative to T-bSiO$_2$ (conceptually shown in graph (a)).

T-bSiO$_2$ (Figure 2). Si-Alk among all cores and depths averaged 88.9 ± 44.5 μmol g^{-1} (±2σ) (range: 53.6–154.4 μmol g^{-1}) (n = 48), while T-bSiO$_2$ released on average 29.2 ± 46.8 μmol g^{-1} (±2σ) (range: 7.8–94.4 μmol g^{-1}) (n = 32).

The pool associated with reactive LSi and refractory bSiO$_2$, Si-NaOH, was isotopically light and the dominant Si pool by mass. δ^{30}Si$_{NaOH}$ averaged −0.54 ± 0.15‰ (±2σ) (range: −0.84‰ and −0.10‰) (n = 48). Additionally, the Si-NaOH mass averaged 920.6 ± 451.4 μmol g^{-1} (±2σ) and ranged between 515.6 and 1,310.1 μmol Si g^{-1}. This sedimentary Si pool was 5–13 times larger than that of Si-HCl and Si-Alk and 20–120 times larger than T-bSiO$_2$ (Figure 2). Si released (μmol g^{-1}) revealed no downcore trends, but this is likely due to the short length of the cores. A table summarizing average δ^{30}Si signals (‰) and Si release (μmol g^{-1}) within each reactive pool can be found in the supporting information (Table S3).

4. Discussion and Conclusions

Si isotopic composition is highly variable among reactive Si pools. The lightest δ^{30}Si nonbiological sedimentary signals reported belong to siliceous precipitates such as hot springs sinters, ranging between −4.0‰ and +0.1‰, (Douthitt, 1982; Geilert et al., 2015) and groundwater silcretes, up to −5.7‰ (Basile-Doelsch, 2006; Basile-Doelsch et al., 2005). The correlation is positive and significant between δ^{30}Si$_{HCl}$ and the biogenic pools (Spearman Rho δ^{30}Si$_{Alk}$: r$_s$ = 0.621, p = 0.010, δ^{30}Si$_{TbSiO2}$: r$_s$ = 0.682, p = 0.004) but negative and insignificantly correlated to the lithogenic signal (δ^{30}Si$_{NaOH}$: r$_s$ = −0.357, p(2-tailed) = 0.174), empirically suggesting biogenic sources for Si-HCl. The isotopically lightest bSiO$_2$ material reported in the ocean belonged to sponge spicules, with δ^{30}Si variations ranging from −5.72‰ to +0.87‰ (Cassarino et al., 2018; De La Rocha, 2003; Frings et al., 2016; Hendry & Robinson, 2012; Sutton et al., 2013; Wang et al., 2019; Wille et al., 2010). While high sediment load likely selects against glass sponges in the Mississippi river delta (Leys et al., 2007), Maldonado et al. (2019) reported that spicule dissolution requires a harsh alkaline total digestion, which implies the Si-HCl pool (leached from 0.1 N HCl) in this study remains unaffected by sedimentary sponge spicules. The discovery of such light material highlights that traditional methods have systematically missed or, more appropriately, not examined this pool; but it questions whether these authigenic products have biased previous measurements by decreasing traditional bSiO$_2$ δ^{30}Si values when samples were not acid cleaned prior to analysis.

The isotopic shift seen between operational pools is large, as δ^{30}Si$_{HCl}$ is 4.5–5‰ lower than the Si liberated in both Si-Alk and T-bSiO$_2$, respectively (Figure 1). Previously, laboratory precipitation synthesis studies (Oelze et al., 2015; Ziegler, Chadwick, Brzezinski, et al., 2005) have demonstrated that solid phase precipitates could be up to 5‰ lower than the solutions in which they were formed. Given that the experimental conditions in these studies (freeze-thaw, pH adjustment, and supersaturated silica) were unlikely applicable to our study sites in a coastal shelf environment, these previous data only demonstrate that the large isotopic fractionation inferred in this study are possible. Whether a single-step authigenic precipitation can explain our observed large isotope shift requires further investigation. Below, we examine processes to determine the evidence for bSiO$_2$ or LSi as sources for these isotopically light silicates.

A fractionation of up to −5‰ is required for bSiO$_2$ to be the acid-leachable Si source (Figure 1). This would be hypothesized to occur in three sequential steps: (1) bSiO$_2$ dissolution, (2) authigenic mineral coating precipitation and oxide adsorption, and (3) multiple cycles of dissolution and reprecipitation. The isotopic fractionation of Si during biogenic silica dissolution has been debated based on material analyzed in both laboratory (Wetzel et al., 2014) and in situ settings (Egan et al., 2012). These studies suggest that overall,

there is little to no isotopic effect during dissolution or early diagenesis on diatom δ^{30}Si signals in bottom sediments. Using the most liberal estimate of isotopic fractionation from dissolution found in the literature (Demarest et al., 2009), that is, −0.55‰, only closes ~10% of the gap between δ^{30}Si in the bSiO$_2$ and the acid-leachable Si. The adsorption of light Si isotopes onto authigenic metal-oxides, specifically Fe-oxy-hydroxides, established a −0.7‰ to −1.6‰ fractionation effect (Delstanche et al., 2009; Opfergelt et al., 2009; Wang et al., 2019) and demonstrates the preferential incorporation of the light Si isotopes into authigenic phases. Ehlert et al. (2016) inferred that the formation of authigenic clays and metal oxides, from dissolving bSiO$_2$, incorporates the lighter isotopes, resulting in a 2‰ fractionation between porewater Si and newly formed materials, leaving pore waters with a heavier isotopic composition. This 2‰ observation is in agreement with many previous studies (Delstanche et al., 2009; Geilert et al., 2014; Ng et al., 2020; Oelze et al., 2014, 2015; Roerdink et al., 2015; Tatzel et al., 2015; Wang et al., 2019). Multistep chemical precipitation/dissolution processes can slowly increase the δ^{30}Si value of interstitial waters and decrease the δ^{30}Si of authigenic phases overtime. This multistep precipitation process increases the discrepancy between the two pools as the amount of detrital material in the sediment increases (Sutton et al., 2018) and therefore results in isotopic shifts ranging between −0.1‰ and −3‰ (Geilert et al., 2014; Oelze et al., 2014, 2015). Given the δ^{30}Si in the Si-Alk and T-bSiO$_2$ pools range between +1.00‰ and +2.69‰, an overestimated 3‰ to 4‰ fractionation effect from this three-step process would imply authigenic Si-HCl δ^{30}Si values of −3‰ to −2‰, which are consistent with the values measured. Thus, fractionation from bSiO$_2$ dissolution and multistep precipitation/dissolution process due to authigenic precipitation and oxide adsorption is possible if each step used an exaggerated fractionation, and this is supported by the strong correlation between δ^{30}Si for Si-HCl and biogenic pools.

Given prior studies, a lower and more realistic fractionation factor would be evoked for the acid-leachable Si to be sourced from LSi and refractory bSiO$_2$ (i.e., Si-NaOH pool). Contrary to bSiO$_2$ dissolution, relatively large fractionation occurs during weathering processes as the δ^{30}Si for secondary clay minerals is 2.95‰ to 0.16‰ lower than the original parent lithogenic silicate material (André et al., 2006; Bern et al., 2010; Cornelis et al., 2010, 2014; Douthitt, 1982; Frings et al., 2016; Georg et al., 2007; Opfergelt & Delmelle, 2012; Wang et al., 2019; Ziegler, Chadwick, Brzezinski, et al., 2005). Additionally, it has previously been established that in the early stages of dissolution of solid lithogenic Si phases, isotopically light Si is released into solution, but the precipitation of silicate phases from this new solution will result in ^{30}Si enrichment in the surrounding solution relative to the new authigenic phase by up to 4‰ (Ziegler, Chadwick, Brzezinski, et al., 2005). δ^{30}Si values for clays range between −3‰ and 0‰ (Delstanche et al., 2009; Georg et al., 2007, 2009; Li et al., 1995; Méheut et al., 2007; Opfergelt & Delmelle, 2012; Savage et al., 2013; Ziegler, Chadwick, Brzezinski, et al., 2005; Ziegler, Chadwick, White, et al., 2005) with lower δ^{30}Si values denoting stronger weathering (Opfergelt et al., 2010). Work by Oelze et al. (2014) supports that such large fractionation from precipitate formation via dissolved LSi is more likely than metal adsorption alone as Si isotopic equilibrium is slow, explaining why light isotopes resulting from early authigenic processes would be carried into diagenesis.

Recently, Chemtob et al. (2015) examined acidic weathering effects on Si isotopes. While in situ measurements in surficial chemical weathering profiles revealed unusual ^{30}Si enrichment (+0.8‰ to 1.36‰) in residual solids, laboratory leaching experiments using fresh basalts and 0.1 M HCl revealed ^{30}Si enriched fluids (1.5–2.3‰), implying ^{30}Si depleted residual solids (Chemtob et al., 2015). Additionally, acidic cleaning experiments using biogenic opal (diatoms and sponge spicules) suggest that there is no impact of cleaning method on final δ^{30}Si signals (Egan et al., 2012; Hendry et al., 2011), implying that HCl leaching effects alone may not drive fractionation changes in authigenic phase signals. Currently, there are no known studies which examine how a mild HCl preleach effects fractionation on natural coastal sediments; this is complicated by the heterogeneous, and often uncharacterized components, within such sediments, especially in river plumes. The Si-NaOH δ^{30}Si reported here lie between −0.84‰ and −0.10‰ (Figure 1), suggesting this pool could be a probable source of the authigenic acid-leachable Si. Although measured in a completely different environment, if we take this fractionation effect from basalt HCl leaching, up to 2.3‰, into account, the gap seen between Si-HCl and Si-NaOH is still not completely accounted for. Previously discussed authigenic mineral coating precipitation and oxide adsorption, of up to 2‰, is necessary to close the gap and account for the entire difference. While the correlation with δ^{30}Si Si-HCl

and Si-NaOH is not strong, metal hydroxide formation and a smaller overall isotopic fractionation (compared to exaggerated fractionation from biogenic sources) suggest the Si-NaOH (LSi) pool could be a Si-HCl source.

The importance of LSi as a source for isotopically light acid-leachable Si pools is bolstered by the disparity among the sedimentary Si pools. The average Si-NaOH (μmol Si g^{-1}) pool is 20-fold larger than that of T-bSiO$_2$ (Figure 2). Although biologic dissolution is more reactive than terrestrially derived silicate minerals (Van Cappellen et al., 2002; Van Cappellen & Qiu, 1997a, 1997b), recent studies demonstrated that particulate LSi mineral dissolution is enhanced in coastal shelf systems along an estuarine gradient via low temperature weathering. Concluding that the physical mass of LSi present serves as a more significant source of dissolved Si to coastal systems and mixing zones than previously assumed (Jeandel & Oelkers, 2015; Jones et al., 2012; Morin et al., 2015). Specifically, Morin et al. (2015) reported surface-area-normalized Si dissolution rates (~10^{-9} mol Si m^{-2} s^{-1}) which exceed those for diatoms (~10^{-10} to 10^{-11} mol Si m^{-2} s^{-1}; Dixit & Van Cappellen, 2002; Saad et al., 2020). Laboratory batch experiments (Oelkers et al., 2011) show that as the dissolved lithogenic material reaches saturation, secondary mineral silicate formation limits the overall effect of low temperature weathering on seawater chemical evolution, which implies that although secondary authigenic mineral precipitation may limit dissolution effects, the addition of an isotopically light distinct particulate phase (e.g., LSi) would be passed on to secondary mineral phases on short time scales (Oelkers et al., 2011). As previously mentioned, the lightest known isotopic Si reservoir is the silicification of silcretes, (Basile-Doelsch, 2006; Basile-Doelsch et al., 2005), which is similar to our Si-HCl pool. These silcrete precipitates form via the precipitation/dissolution of secondary lithogenic quartz in a radically different (mostly arid) environmental setting but support that the dissolution and precipitation of isotopically depleted LSi materials may be a Si source for the Si-HCl pool. Given this implication, we feel this area merits future study.

The data presented also demonstrate that there are resolvable isotopic differences between the traditional DeMaster (1981) method (T-bSiO$_2$) and Michalopoulos and Aller's (2004) reactive bSiO$_2$ pool (Si-Alk). δ^{30}Si$_{Alk}$ represents mixed signatures from bSiO$_2$, metal oxides, and authigenic clays, while δ^{30}Si$_{T-bSiO2}$ just reveals bSiO$_2$ values, most likely from diatoms (Maldonado et al., 2019). This is largely attributed to the T-bSiO$_2$ treatment (DeMaster, 1981) not fully dissolving newly formed authigenic metal oxides and releasing the Si sorbed to them (Michalopoulos & Aller, 2004). Given both the isotopic and mass differential between the T-bSiO$_2$ and Si-Alk pools, this suggests the excess Si released from authigenically altered bSiO$_2$ (i.e., Si-Alk mass exceeding T-bSiO$_2$ mass) has a different isotopic composition. Because the Si-Alk isotopic composition is affected by both the T-bSiO$_2$ and the excess liberated Si (Si-Alk – T-bSiO$_2$), a mass balance approach can be used to determine the isotopic composition of the authigenically altered bSiO$_2$ (termed Apparent Si-Alk, Figure 3). Apparent Si-Alk was, on average, 0.56‰ higher than T-bSiO$_2$. More importantly, this implies that the bSiO$_2$ substrate which serves as a template for authigenic products is isotopically heavy (δ^{30}Si > 2.0‰). Regardless of differences, the isotopic composition of the bSiO$_2$ phase seems to be unaffected by secondary authigenic precipitation (i.e., structural isotopic exchange), which implies that if care is taken to extract a clean bSiO$_2$ phase from sediments, isotopic records are reliable.

The Apparent Si-Alk analysis suggests that diatom silica serves an integral role during authigenesis, independent of whether it is the main Si source for Si-HCl. Our finding that the Apparent Si-Alk pool is isotopically heavier than the T-bSiO$_2$ pool, which has not undergone authigenic modification, suggests that the Apparent Si-Alk material has a water column source where Si (OH)$_4$ can be isotopically heavy. This underscores the power of analyzing multiple reactive pools, as this finding would have been masked without data among both T- bSiO$_2$ and Si-Alk pools. Water-column diatoms can consume Si (OH)$_4$ concentrations to virtual exhaustion in the Mississippi River plume (Nelson & Dortch, 1996), and diatoms are isotopically heavier than other marine siliceous organisms (Sutton et al., 2018). This is consistent with electron microscopy data showing that authigenic phases coat diatom bSiO$_2$ (Loucaides, Behrends, et al., 2010; Loucaides, Michalopoulos, et al., 2010; Michalopoulos et al., 2000; Michalopoulos & Aller, 2004). Additionally, in this region, there has been a threefold increase of diatom bSiO$_2$ in sediments over the last 50 years (Parsons et al., 2002; Turner et al., 2008; Turner & Rabalais, 1994). This increase in regional sediment bSiO$_2$ has occurred contemporaneous with eutrophication in the region. Therefore, if diatoms are the main substrate for sedimentary authigenic products, it is probable that anthropogenic effects on

the Louisiana Shelf, which have stimulated sedimentary $bSiO_2$ accumulation, may also have facilitated additional sequestration of both sedimentary Si and cations (Isson & Planavsky, 2018; Krissansen-Totton & Catling, 2020; Mackenzie & Kump, 1995; Michalopoulos & Aller, 1995).

Overall, coupling $\delta^{30}Si$ with sequential leach-digestion methods provides a new approach to examine the sedimentary silica phases in biogeochemically important regions (e.g., river plumes). Using $\delta^{30}Si$ signals, we infer two pathways for formation of acid-leachable reactive silica and suggest LSi (with some refractory $bSiO_2$) requires fewer and less exaggerated fractionation steps than $bSiO_2$, although $bSiO_2$ $\delta^{30}Si$ is well correlated to that of the acid-leachable pool. Furthermore, we have shown independently (without aid of electron microscopy) that a majority of the water-column diatom $bSiO_2$ in these sediments is altered rapidly (on the order of months) during early diagenesis in the surface sediments, as sediment deposition in the Mississippi delta can be variable (upward of 10 cm a^{-1}) (Adhikari et al., 2016; Chen et al., 2005; Devereux et al., 2019). Given eutrophication in the river waters feeding this system, which have led to increasing $bSiO_2$ in regional sediments, the strength of this process as an elemental sink may have increased in the last half century.

Data Availability Statement

All original data are shown in the paper and are also available publicly at the Biological and Chemical Oceanography Data Management Office, Project 712667 (doi:10.1575/1912/bco-dmo.786508.1).

Conflict of Interest

The authors declare no competing interests.

References

Adhikari, P. L., Maiti, K., Overton, E. B., Rosenheim, B. E., & Marx, B. D. (2016). Distributions and accumulation rates of polycyclic aromatic hydrocarbons in the northern Gulf of Mexico sediments. *Environmental Pollution*, *212*, 413–423. https://doi.org/10.1016/j.envpol.2016.01.064

André, L., Cardinal, D., Alleman, L. Y., & Moorbath, S. (2006). Silicon isotopes in ~3.8 Ga West Greenland rocks as clues to the Eoarchaean supracrustal Si cycle. *Earth and Planetary Science Letters*, *245*(1–2), 162–173. https://doi.org/10.1016/j.epsl.2006.02.046

Basile-Doelsch, I. (2006). Si stable isotopes in the Earth's surface: A review. *Journal of Geochemical Exploration*, *88*(1–3) SPEC. ISS, 252–256. https://doi.org/10.1016/j.gexplo.2005.08.050

Basile-Doelsch, I., Meunier, J. D., & Parron, C. (2005). Another continental pool in the terrestrial silicon cycle. *Nature*, *433*(7024), 399–402. https://doi.org/10.1038/nature03217

Bern, C. R., Brzezinski, M. A., Beucher, C., Ziegler, K., & Chadwick, O. A. (2010). Weathering, dust, and biocycling effects on soil silicon isotope ratios. *Geochimica et Cosmochimica Acta*, *74*(3), 876–889. https://doi.org/10.1016/j.gca.2009.10.046

Brzezinski, M. A., & Nelson, D. M. (1986). A solvent extraction method for the colorimetric determination of nanomolar concentrations of silicic acid in seawater. *Marine Chemistry*, *19*(2), 139–151. https://doi.org/10.1016/0304-4203(86)90045-9

Cardinal, D., Alleman, L. Y., De Jong, J., Ziegler, K., & André, L. (2003). Isotopic composition of silicon measured by multicollector plasma source mass spectrometry in dry plasma mode. *Journal of Analytical Atomic Spectrometry*, *18*(3), 213–218. https://doi.org/10.1039/b210109b

Cassarino, L., Coath, C. D., Xavier, J. R., & Hendry, K. R. (2018). Silicon isotopes of deep sea sponges: New insights into biomineralisation and skeletal structure. *Biogeosciences*, *15*(22), 6959–6977. https://doi.org/10.5194/bg-15-6959-2018

Chemtob, S. M., Rossman, G. R., Young, E. D., Ziegler, K., Moynier, F., Eiler, J. M., & Hurowitz, J. A. (2015). Silicon isotope systematics of acidic weathering of fresh basalts, Kilauea volcano, Hawai'i. *Geochimica et Cosmochimica Acta*, *169*, 63–81. https://doi.org/10.1016/j.gca.2015.07.026

Chen, N., Bianchi, T. S., & McKee, B. A. (2005). Early diagenesis of chloropigment biomarkers in the lower Mississippi River and Louisiana shelf: Implications for carbon cycling in a river-dominated margin. *Marine Chemistry*, *93*(2–4), 159–177. https://doi.org/10.1016/j.marchem.2004.08.005

Cornelis, J. T., Delvaux, B., Cardinal, D., André, L., Ranger, J., & Opfergelt, S. (2010). Tracing mechanisms controlling the release of dissolved silicon in forest soil solutions using Si isotopes and Ge/Si ratios. *Geochimica et Cosmochimica Acta*, *74*(14), 3913–3924. https://doi.org/10.1016/j.gca.2010.04.056

Cornelis, J. T., Weis, D., Lavkulich, L., Vermeire, M. L., Delvaux, B., & Barling, J. (2014). Silicon isotopes record dissolution and re-precipitation of pedogenic clay minerals in a podzolic soil chronosequence. *Geoderma*, *235-236*, 19–29. https://doi.org/10.1016/j.geoderma.2014.06.023

De La Rocha, C. L. (2003). Silicon isotope fractionation by marine sponges and the reconstruction of the silicon isotope composition of ancient deep water. *Geology*, *31*(5), 423–426. https://doi.org/10.1130/0091-7613(2003)031<0423:SIFBMS>2.0.CO;2

Delstanche, S., Opfergelt, S., Cardinal, D., Elsass, F., André, L., & Delvaux, B. (2009). Silicon isotopic fractionation during adsorption of aqueous monosilicic acid onto iron oxide. *Geochimica et Cosmochimica Acta*, *73*(4), 923–934. https://doi.org/10.1016/j.gca.2008.11.014

Demarest, M. S., Brzezinski, M. A., & Beucher, C. P. (2009). Fractionation of silicon isotopes during biogenic silica dissolution. *Geochimica et Cosmochimica Acta*, *73*(19), 5572–5583. https://doi.org/10.1016/j.gca.2009.06.019

DeMaster, D. J. (1981). The supply and accumulation of silica in the marine environment. *Geochimica et Cosmochimica Acta*, *45*(10), 1715–1732. https://doi.org/10.1016/0016-7037(81)90006-5

Devereux, R., Lehrter, J. C., Cicchetti, G., Beddick, D. L. Jr., Yates, D. F., Jarvis, B. M., et al. (2019). Spatially variable bioturbation and physical mixing drive the sedimentary biogeochemical seascape in the Louisiana continental shelf hypoxic zone. *Biogeochemistry*, *143*(2), 151–169. https://doi.org/10.1007/s10533-019-00539-8

Dixit, S., & Van Cappellen, P. (2002). Surface chemistry and reactivity of biogenic silica. *Geochimica et Cosmochimica Acta*, *66*(14), 2559–2568. https://doi.org/10.1016/S0016-7037(02)00854-2

Douthitt, C. B. (1982). The geochemistry of the stable isotopes of silicon. *Geochimica et Cosmochimica Acta*, *46*(8), 1449–1458. https://doi.org/10.1016/0016-7037(82)90278-2

Egan, K. E., Rickaby, R. E. M., Leng, M. J., Hendry, K. R., Hermoso, M., Sloane, H. J., et al. (2012). Diatom silicon isotopes as a proxy for silicic acid utilisation: A Southern Ocean core top calibration. *Geochimica et Cosmochimica Acta*, *96*, 174–192. https://doi.org/10.1016/j.gca.2012.08.002

Ehlert, C., Doering, K., Wallmann, K., Scholz, F., Sommer, S., Grasse, P., et al. (2016). Stable silicon isotope signatures of marine pore waters—Biogenic opal dissolution versus authigenic clay mineral formation. *Geochimica et Cosmochimica Acta*, *191*, 102–117. https://doi.org/10.1016/j.gca.2016.07.022

Frings, P. J., Clymans, W., Fontorbe, G., De La Rocha, C. L., & Conley, D. J. (2016). The continental Si cycle and its impact on the ocean Si isotope budget. *Chemical Geology*, *425*, 12–36. https://doi.org/10.1016/j.chemgeo.2016.01.020

Frings, P. J., Clymans, W., Fontorbe, G., Gray, W., Chakrapani, G., Conley, D. J., & De La Rocha, C. (2015). Silicate weathering in the Ganges alluvial plain. *Earth and Planetary Science Letters*, *427*, 136–148. https://doi.org/10.1016/j.epsl.2015.06.049

Frings, P. J., de la Rocha, C., Struyf, E., van Pelt, D., Schoelynck, J., Hudson, M. M., et al. (2014). Tracing silicon cycling in the Okavango Delta, a sub-tropical flood-pulse wetland using silicon isotopes. *Geochimica et Cosmochimica Acta*, *142*, 132–148. https://doi.org/10.1016/j.gca.2014.07.007

Geilert, S., Vroon, P. Z., Keller, N. S., Gudbrandsson, S., Stefánsson, A., & van Bergen, M. J. (2015). Silicon isotope fractionation during silica precipitation from hot-spring waters: Evidence from the Geysir geothermal field, Iceland. *Geochimica et Cosmochimica Acta*, *164*, 403–427. https://doi.org/10.1016/j.gca.2015.05.043

Geilert, S., Vroon, P. Z., Roerdink, D. L., Van Cappellen, P., & van Bergen, M. J. (2014). Silicon isotope fractionation during abiotic silica precipitation at low temperatures: Inferences from flow-through experiments. *Geochimica et Cosmochimica Acta*, *142*(1), 95–114. https://doi.org/10.1016/j.gca.2014.07.003

Georg, R. B., Reynolds, B. C., Frank, M., & Halliday, A. N. (2006). New sample preparation techniques for the determination of Si isotopic compositions using MC-ICPMS. *Chemical Geology*, *235*(1–2), 95–104. https://doi.org/10.1016/j.chemgeo.2006.06.006

Georg, R. B., Reynolds, B. C., West, A. J., Burton, K. W., & Halliday, A. N. (2007). Silicon isotope variations accompanying basalt weathering in Iceland. *Earth and Planetary Science Letters*, *261*(3–4), 476–490. https://doi.org/10.1016/j.epsl.2007.07.004

Georg, R. B., Zhu, C., Reynolds, B. C., & Halliday, A. N. (2009). Stable silicon isotopes of groundwater, feldspars, and clay coatings in the Navajo Sandstone aquifer, Black Mesa, Arizona, USA. *Geochimica et Cosmochimica Acta*, *73*(8), 2229–2241. https://doi.org/10.1016/j.gca.2009.02.005

Hendry, K. R., Leng, M. J., Robinson, L. F., Sloane, H. J., Blusztjan, J., Rickaby, R. E. M., et al. (2011). Silicon isotopes in Antarctic sponges: An interlaboratory comparison. *Antarctic Science*, *23*(1), 34–42. https://doi.org/10.1017/S0954102010000593

Hendry, K. R., & Robinson, L. F. (2012). The relationship between silicon isotope fractionation in sponges and silicic acid concentration: Modern and core-top studies of biogenic opal. *Geochimica et Cosmochimica Acta*, *81*, 1–12. https://doi.org/10.1016/j.gca.2011.12.010

Hughes, H. J., Delvigne, C., Korntheuer, M., De Jong, J., André, L., & Cardinal, D. (2011). Controlling the mass bias introduced by anionic and organic matrices in silicon isotopic measurements by MC-ICP-MS. *Journal of Analytical Atomic Spectrometry*, *26*(9), 1892–1896. https://doi.org/10.1039/c1ja10110b

Isson, T. T., & Planavsky, N. J. (2018). Reverse weathering as a long-term stabilizer of marine pH and planetary climate. *Nature*, *560*(7719), 471–475. https://doi.org/10.1038/s41586-018-0408-4

Jeandel, C., & Oelkers, E. H. (2015). The influence of terrigenous particulate material dissolution on ocean chemistry and global element cycles. *Chemical Geology*, *395*, 50–66. https://doi.org/10.1016/j.chemgeo.2014.12.001

Jones, M. T., Pearce, C. R., & Oelkers, E. H. (2012). An experimental study of the interaction of basaltic riverine particulate material and seawater. *Geochimica et Cosmochimica Acta*, *77*, 108–120. https://doi.org/10.1016/j.gca.2011.10.044

Kamatani, A., & Oku, O. (2000). Measuring biogenic silica in marine sediments. *Marine Chemistry*, *68*(3), 219–229. https://doi.org/10.1016/s0304-4203(99)00079-1

Krause, J. W., Darrow, E. S., Pickering, R. A., Carmichael, R. H., Larson, A. M., & Basaldua, J. L. (2017). Reactive silica fractions in coastal lagoon sediments from the northern Gulf of Mexico. *Continental Shelf Research*, *151*, 8–14. https://doi.org/10.1016/j.csr.2017.09.014

Krissansen-Totton, J., & Catling, D. C. (2020). A coupled carbon-silicon cycle model over earth history: Reverse weathering as a possible explanation of a warm mid-Proterozoic climate. *Earth and Planetary Science Letters*, *537*, 116181. https://doi.org/10.1016/j.epsl.2020.116181

Leys, S. P., Mackie, G. O., & Reiswig, H. M. (2007). The biology of glass sponges. *Advances in Marine Biology*, *52*(06), 1–145. https://doi.org/10.1016/S0065-2881(06)52001-2

Li, Y., Ding, T., & Wan, D. (1995). Experimental study of silicon isotope dynamic fractionation and its application in geology. *Chinese Journal of Geochemistry*, *14*(3), 212–219. https://doi.org/10.1007/BF02842044

Loucaides, S., Behrends, T., & Van Cappellen, P. (2010). Reactivity of biogenic silica: Surface versus bulk charge density. *Geochimica et Cosmochimica Acta*, *74*(2), 517–530. https://doi.org/10.1016/j.gca.2009.10.038

Loucaides, S., Michalopoulos, P., Presti, M., Koning, E., Behrends, T., & Van Cappellen, P. (2010). Seawater-mediated interactions between diatomaceous silica and terrigenous sediments: Results from long-term incubation experiments. *Chemical Geology*, *270*(1–4), 68–79. Retrieved from. https://doi.org/10.1016/j.chemgeo.2009.11.006

Mackenzie, F., & Kump, L. R. (1995). Reverse weathering, clay mineral formation, and oceanic element cycles. *Science*, *270*(5236), 586–587. https://doi.org/10.1126/science.270.5236.586

Maldonado, M., López-Acosta, M., Sitjà, C., García-Puig, M., Galobart, C., Ercilla, G., & Leynaert, A. (2019). Sponge skeletons as an important sink of silicon in the global oceans. *Nature Geoscience*, *12*(10), 815–822. https://doi.org/10.1038/s41561-019-0430-7

Méheut, M., Lazzeri, M., Balan, E., & Mauri, F. (2007). Equilibrium isotopic fractionation in the kaolinite, quartz, water system: Prediction from first-principles density-functional theory. *Geochimica et Cosmochimica Acta*, *71*(13), 3170–3181. https://doi.org/10.1016/j.gca.2007.04.012

Michalopoulos, P., & Aller, R. C. (1995). Rapid clay mineral formation in Amazon delta sediments: Reverse weathering and oceanic elemental cycles. *Science*, *270*(5236), 614–617. https://doi.org/10.1126/science.270.5236.614

Michalopoulos, P., & Aller, R. C. (2004). Early diagenesis of biogenic silica in the Amazon delta: Alteration, authigenic clay formation, and storage. *Geochimica et Cosmochimica Acta*, *68*(5), 1061–1085. https://doi.org/10.1016/j.gca.2003.07.018

Michalopoulos, P., Aller, R. C., & Reeder, R. J. (2000). Conversion of diatoms to clays during early diagenesis in tropical, continental shell muds. *Geology*, *28*(12), 1095–1098. https://doi.org/10.1130/0091-7613(2000)028<1095:CODTCD>2.3.CO;2

Morin, G. P., Vigier, N., & Verney-Carron, A. (2015). Enhanced dissolution of basaltic glass in brackish waters: Impact on biogeochemical cycles. *Earth and Planetary Science Letters*, *417*, 1–8. https://doi.org/10.1016/j.epsl.2015.02.005

Nelson, D. M., & Dortch, Q. (1996). Slicic acid depletion and silicon limitation in the plume of the Mississippi River: Evidence from kinetic studies in spring and summer. *Marine Ecology Progress Series*, *136*, 163–178. https://doi.org/10.3354/meps136163

Ng, H. C., Cassarino, L., Pickering, R. A., Woodward, E. M. S., Hammond, S. J., & Hendry, K. R. (2020). Sediment efflux of silicon on the Greenland margin and implications for the marine silicon cycle. *Earth and Planetary Science Letters*, *529*, 115877. https://doi.org/10.1016/j.epsl.2019.115877

Oelkers, E. H., Gislason, S. R., Eiriksdottir, E. S., Jones, M., Pearce, C. R., & Jeandel, C. (2011). The role of riverine particulate material on the global cycles of the elements. *Applied Geochemistry*, *26*(SUPPL.), S365–S369. https://doi.org/10.1016/j.apgeochem.2011.03.062

Oelze, M., von Blanckenburg, F., Bouchez, J., Hoellen, D., & Dietzel, M. (2015). The effect of Al on Si isotope fractionation investigated by silica precipitation experiments. *Chemical Geology*, *397*, 94–105. https://doi.org/10.1016/j.chemgeo.2015.01.002

Oelze, M., von Blanckenburg, F., Hoellen, D., Dietzel, M., & Bouchez, J. (2014). Si stable isotope fractionation during adsorption and the competition between kinetic and equilibrium isotope fractionation: Implications for weathering systems. *Chemical Geology*, *380*, 161–171. https://doi.org/10.1016/j.chemgeo.2014.04.027

Opfergelt, S., Cardinal, D., André, L., Delvigne, C., Bremond, L., & Delvaux, B. (2010). Variations of δ^{30}Si and Ge/Si with weathering and biogenic input in tropical basaltic ash soils under monoculture. *Geochimica et Cosmochimica Acta*, *74*(1), 225–240. https://doi.org/10.1016/j.gca.2009.09.025

Opfergelt, S., de Bournonville, G., Cardinal, D., André, L., Delstanche, S., & Delvaux, B. (2009). Impact of soil weathering degree on silicon isotopic fractionation during adsorption onto iron oxides in basaltic ash soils, Cameroon. *Geochimica et Cosmochimica Acta*, *73*(24), 7226–7240. https://doi.org/10.1016/j.gca.2009.09.003

Opfergelt, S., & Delmelle, P. (2012). Silicon isotopes and continental weathering processes: Assessing controls on Si transfer to the ocean. *Comptes Rendus - Geoscience*, *344*(11–12), 723–738. https://doi.org/10.1016/j.crte.2012.09.006

Parsons, M. L., Dortch, Q., & Turner, R. E. (2002). Sedimentological evidence of an increase in *Pseudo-nitzschia* (Bacillariophyceae) abundance in response to coastal eutrophication. *Limnology and Oceanography*, *47*(2), 551–558. https://doi.org/10.4319/lo.2002.47.2.0551

Presti, M., & Michalopoulos, P. (2008). Estimating the contribution of the authigenic mineral component to the long-term reactive silica accumulation on the western shelf of the Mississippi River Delta. *Continental Shelf Research*, *28*(6), 823–838. https://doi.org/10.1016/j.csr.2007.12.015

Qin, Y. C., Weng, H. X., Jin, H., Chen, J., & Tian, R. X. (2012). Estimation of authigenic alteration of biogenic and reactive silica in Pearl River estuarine sediments using wet-chemical digestion methods. *Environmental Earth Sciences*, *65*(6), 1855–1864. https://doi.org/10.1007/s12665-011-1168-8

Ragueneau, O., Savoye, N., Del Amo, Y., Cotten, J., Tardiveau, B., & Leynaert, A. (2005). A new method for the measurement of biogenic silica in suspended matter of coastal waters: Using Si:Al ratios to correct for the mineral interference. *Continental Shelf Research*, *25*(5-6), 697–710. https://doi.org/10.1016/j.csr.2004.09.017

Rahman, S., Aller, R. C., & Cochran, J. K. (2016). Cosmogenic ^{32}Si as a tracer of biogenic silica burial and diagenesis: Major deltaic sinks in the silica cycle. *Geophysical Research Letters*, *43*, 7124–7132. https://doi.org/10.1002/2016GL069929

Rahman, S., Aller, R. C., & Cochran, J. K. (2017). The missing silica sink: Revisiting the marine sedimentary Si cycle using cosmogenic ^{32}Si. *Global Biogeochemical Cycles*, *31*, 1559–1578. https://doi.org/10.1002/2017GB005746

Rahman, S., Tamborski, J. J., Charette, M. A., & Cochran, J. K. (2019). Dissolved silica in the subterranean estuary and the impact of submarine groundwater discharge on the global marine silica budget. *Marine Chemistry.*, *208*, 29–42. https://doi.org/10.1016/j.marchem.2018.11.006

Reynolds, B. C., Aggarwal, J., André, L., Baxter, D., Beucher, C., Brzezinski, M. A., et al. (2007). An inter-laboratory comparison of Si isotope reference materials. *Journal of Analytical Atomic Spectrometry*, *22*(5), 561–568. https://doi.org/10.1039/b616755a

Roerdink, D. L., van den Boorn, S. H. J. M., Geilert, S., Vroon, P. Z., & van Bergen, M. J. (2015). Experimental constraints on kinetic and equilibrium silicon isotope fractionation during the formation of non-biogenic chert deposits. *Chemical Geology*, *402*, 40–51. https://doi.org/10.1016/j.chemgeo.2015.02.038

Saad, E. M., Pickering, R. A., Shoji, K., Hossain, M. I., Glover, T. G., Krause, J. W., & Tang, Y. (2020). Effect of cleaning methods on the dissolution of diatom frustules. *Marine Chemistry*, *224*, 103826. https://doi.org/10.1016/j.marchem.2020.103826

Savage, P. S., Georg, R. B., Williams, H. M., & Halliday, A. N. (2013). The silicon isotope composition of the upper continental crust. *Geochimica et Cosmochimica Acta*, *109*, 384–399. https://doi.org/10.1016/j.gca.2013.02.004

Sutton, J. N., André, L., Cardinal, D., Conley, D. J., de Souza, G. F., Dean, J., et al. (2018). A review of the stable isotope bio-tgeochemistry of the global silicon cycle and its associated trace elements. *Frontiers in Earth Science*, *5*(112). https://doi.org/10.3389/feart.2017.00112

Sutton, J. N., Varela, D. E., Brzezinski, M. A., & Beucher, C. P. (2013). Species-dependent silicon isotope fractionation by marine diatoms. *Geochimica et Cosmochimica Acta*, *104*, 300–309. https://doi.org/10.1016/j.gca.2012.10.057

Tatzel, M., von Blanckenburg, F., Oelze, M., Schuessler, J. A., & Bohrmann, G. (2015). The silicon isotope record of early silica diagenesis. *Earth and Planetary Science Letters*, *428*, 293–303. https://doi.org/10.1016/j.epsl.2015.07.018

Tréguer, P., & De La Rocha, C. L. (2013). The world ocean silica cycle. *Annual Review of Marine Science*, *5*(1), 477–501. https://doi.org/10.1146/annurev-marine-121211-172346

Trower, E. J., & Fischer, W. W. (2019). Precambrian Si isotope mass balance, weathering, and the significance of the authigenic clay silica sink. *Sedimentary Geology*, *384*, 1–11. https://doi.org/10.1016/j.sedgeo.2019.02.008

Turner, R. E., & Rabalais, N. N. (1994). Coastal eutrophication near the Mississippi river delta. *Nature*, *368*(6472), 619–621. https://doi.org/10.1038/368619a0

Turner, R. E., Rabalais, N. N., & Justic, D. (2008). Gulf of Mexico hypoxia: Alternate states and a legacy. *Environmental Science and Technology*, *42*(7), 2323–2327. https://doi.org/10.1021/es071617k

Van Cappellen, P., Dixit, S., & van Beusekom, J. (2002). Biogenic silica dissolution in the oceans: Reconciling experimental and field-based dissolution rates. *Global Biogeochemical Cycles*, *16*(4), 1075. https://doi.org/10.1029/2001GB001431

Van Cappellen, P., & Qiu, L. (1997a). Biogenic silica dissolution in sediments of the Southern Ocean. I. Solubility. *Deep-Sea Research Part II: Topical Studies in Oceanography*, *44*(5), 1109–1128. https://doi.org/10.1016/S0967-0645(96)00113-0

Van Cappellen, P., & Qiu, L. (1997b). Biogenic silica dissolution in sediments of the Southern Ocean. *II. Kinetics. Deep-Sea Research Part II: Topical Studies in Oceanography*, *44*(5), 1129–1149. https://doi.org/10.1016/S0967-0645(96)00112-9

Wang, C., Zhu, H., Wang, P., Hou, J., Ao, Y., & Fan, X. (2015). Early diagenetic alterations of biogenic and reactive silica in the surface sediment of the Yangtze Estuary. *Continental Shelf Research*, *99*, 1–11. https://doi.org/10.1016/j.csr.2015.03.003

Wang, W., Wei, H. Z., Jiang, S. Y., Liu, X., Lei, F., Lin, Y. B., & Zhao, Y. (2019). Silicon isotope geochemistry: Fractionation linked to silicon complexations and its geological applications. *Molecules*, *24*(7), 1415. https://doi.org/10.3390/molecules24071415

Wetzel, F., de Souza, G. F., & Reynolds, B. C. (2014). What controls silicon isotope fractionation during dissolution of diatom opal? *Geochimica et Cosmochimica Acta*, *131*, 128–137. https://doi.org/10.1016/j.gca.2014.01.028

Wille, M., Sutton, J., Ellwood, M. J., Sambridge, M., Maher, W., Eggins, S., & Kelly, M. (2010). Silicon isotopic fractionation in marine sponges: A new model for understanding silicon isotopic variations in sponges. *Earth and Planetary Science Letters*, *292*(3–4), 281–289. https://doi.org/10.1016/j.epsl.2010.01.036

Ziegler, K., Chadwick, O. A., Brzezinski, M. A., & Kelly, E. F. (2005). Natural variations of δ30Si ratios during progressive basalt weathering, Hawaiian Islands. *Geochimica et Cosmochimica Acta*, *69*(19), 4597–4610. https://doi.org/10.1016/j.gca.2005.05.008

Ziegler, K., Chadwick, O. A., White, A. F., & Brzezinski, M. A. (2005). δ^{30}Si systematics in a granitic saprolite, Puerto Rico. *Geology*, *33*(10), 817–820. https://doi.org/10.1130/G21707.1